A Coupled Atmospheric and Wave Modeling System for Storm Simulations

Du, Jianting; Larsén, Xiaoli Guo; Bolanos, R.

Published in:
Proceedings of EWEA Offshore 2015 Conference

Publication date:
2015

Document Version
Publisher's PDF, also known as Version of record

A Coupled Atmospheric and Wave Modeling System for Storm Simulations

J. Du[1], X.G. Larsén[1], R. Bolaños[2]

Wind Energy Department, DTU, Risø Campus, Roskilde, Denmark
jitd@dtu.dk
[2] DHI, DK-2907 Hørsholm, Denmark

Abstract. This study aims at improving the simulation of wind and waves during storms in connection with wind turbine design and operations in coastal areas. For this particular purpose, we investigated the Coupled-Ocean-Atmosphere-Wave-Sediment Transport (COAWST) Modeling System which couples the Weather Research and Forecasting (WRF) Model with the third-generation ocean wave model–SWAN. This study investigates mainly two issues: spatial resolution and the wind-wave interface parameter – roughness length(z_0). To study the impact of resolution, the nesting function for both WRF and SWAN is used, with spatial resolution ranging from $25km$ to $2km$. Meanwhile, the atmospheric forcing data of different spatial resolution, with one about $100km$ (FNL) and the other about $38km$ (CFSR) are both used. In addition, bathymatry data of diffferent resolutions ($1arc-minute$ and $30arc-seconds$) are used. We used three approaches to parametrize z_0. The results are validated through QuikScat data and point measurements from an open ocean site Ekofisk and a coastal, relatively shallow water site Horns Rev. It is found that the modeling system captures in general better strong wind and strong wave characteristics for open ocean condition than for the coastal condition. With the current model setup, using high spatial resolution gives better results for strong winds both for the open ocean and coastal sites. The significant wave height (H_{m0}) is very sensitive to the model resolution and bathymetry data for the coastal zone. In addition, using Janssen (1991) z_0 expression gives better results of the significant wave hight under high sea state conditions.

Keywords: Atmosphere and wave coupling, Storm, Coastal zone, High resolution

1 Introduction

Wind and wave forecast at coastal zones during storms are important for the offshore wind turbine design and wind power operations. Zambon et al. (2014) pointed out that the inaccuracy of uncoupled wave models are due to the coarse-grid spacing of the wind fields and the treatment of surface roughness as a function of local wind vector. The objective of the present study is to understand the sensitivity of the spatical resolution and to evaluate the role of wind-wave interation in coastal areas. The outline of this paper is as follows: The coupling system, the methodology of momentum flux calculation, and the experimental design are described in section 2; the results are discussed in section 3; and a conclusion is presented in section 4.

2 Model and Experiments Description

The Coupled Ocean-Atmosphere-Wave-Sediment-Transport (COAWST) Modeling System (Warner et al., 2010) was used in this study. The modeling system consists of four model components: the Regional Ocean Modeling System (ROMS) (Shchepetkin & McWilliams, 2005), the Weather Research and Forecasting (WRF) model (Skamarock et al., 2005), the Simulating Waves Nearshore (SWAN), and the Community Sediment Transport Model (CSTM) (Warner et al. 2008). Data exchange between models are handled by the Model Coupling Toolkit (MCT) (Larson et al., 2005) and the remapping

weights between different grid structures are calculated by SCRIP—A Spherical Coordinate Remapping and Interpolation Package. The detailed descriptions of the coupling methodology is presented in Warner et al. (2008, 2010). In this study, we focus on the influence of the ocean surface waves on the atmospheric modeling. So the ROMS model was turned off.

2.1 Roughness length expressions

Fields exchanged in the two-way coupled system are shown in Fig.1. WRF transfers wind speeds at $10m$ above the sea surface (u_{10}, v_{10}) to SWAN, and SWAN passes back significant wave height(H_{m0}), wave length (L_p) and wave period (T_p) at the peak frequency of the wave spectrum. In COAWST version 3.1, there are three methods for the parameterization of z_0 (Olabarrieta et al., 2012), including Taylor & Yelland(2001), Oost et al.(2002), and Drennan et al.(2005). In the present study, two more methods are implemented (Bolaños et al., 2014). One is from Fan et al. (2012) in which the Charnock parameter is fitted by wave age, where the fitting constants are functions of $10m$ wind speed. The other is from Janssen (1991) in which the z_0 is directly transfered from the wave model.

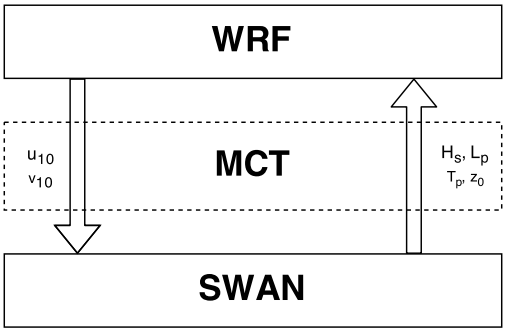

Fig. 1. Diagram of fields exchanged in the WRF-SWAN two way online coupling system

2.2 Experimental design

The model domains as well as the measurements locations are shown in Fig.2. Both of WRF and SWAN are two-domain nested. The resolution of WRF outer and inner domains are $25km$ and $5km$ respectively, with 41 vertical levels. The initial and boundary conditions are from NCEP FNL (Final) Operational Global Analysis data on $1-degree$ grids. The planetary boundary laryer was modeled with the Mellor-Yamada Nakanishi Niino (MYNN) (Nakanishi & Niino, 2009) closure scheme. The horizontal resolution of SWAN outer and inner domain is $\sim 12km$ and $\sim 6km$ respecitively. The bathymetry data is from ETOPO $1arc-minute$ Global relief model (Amante et al. 2009). SWAN initials from zero spectra and its open boundaries are set to Jonswap spectrum with $H_{m0} = 2m$, $T_p = 8s$. Directional space was utilized with 36 directional bins. And the frequency resolution is equal to $\triangle f = 0.1435f$ between $0.04Hz$ and $1Hz$. The wind input and the white-capping dissipation source function are based on Janssen (1991,1992). Data exchange frequency between WRF and SWAN is once every 5 minutes. Three storms were studied representing different wind directions and onshore/offshore conditions. Fig.4 gives a glance of the respective structure of the storms. The first one is from $22^{nd}Dec.2002$ to $25^{th}Dec.2002$, which is an offshore case at Horns Rev. The wind direction is mainly from southeast

(SE02). The second one is from $14^{th}Dec.$2003 to $16^{th}Dec.$2003, which is an onshore case at Horns Rev. The wind direction is mainly from northwest (NW03). The third one is from $19^{th}Mar.$2004 to $23^{rd}Mar.$2004, which is another onshore case at Horns Rev. The wind direction is mainly from southwest (SW04). Table 1, EXP1-EXP6 is a summary of the model settings for the experiments.

To examine the impact of spatial resolution, in addition to the model setup of the spatial resolution ranging from $25km$ to $2km$ (Table 1, EXP7-EXP9), we also used a relatively high resolution large scale forcing for WRF. High resolution bathymetry data are also used. Accordingly, a refined three-domain nested experiment was designed for strom NW03(Fig.3). The horizontal resolution of WRF are from $18km$ to $6km$ to $2km$, and the horizontal resolution for SWAN are from $\sim 12km$ to $\sim 4km$ to $\sim 1.3km$. Initial and boundary conditions for WRF are from NCEP Climate Forecast System Reanalysis (CFSR) data on about $38km$ grids. Bathymetry for SWAN is from GEBCO (Ioc, I. ,2008) $30arc-second$ global gridded data.

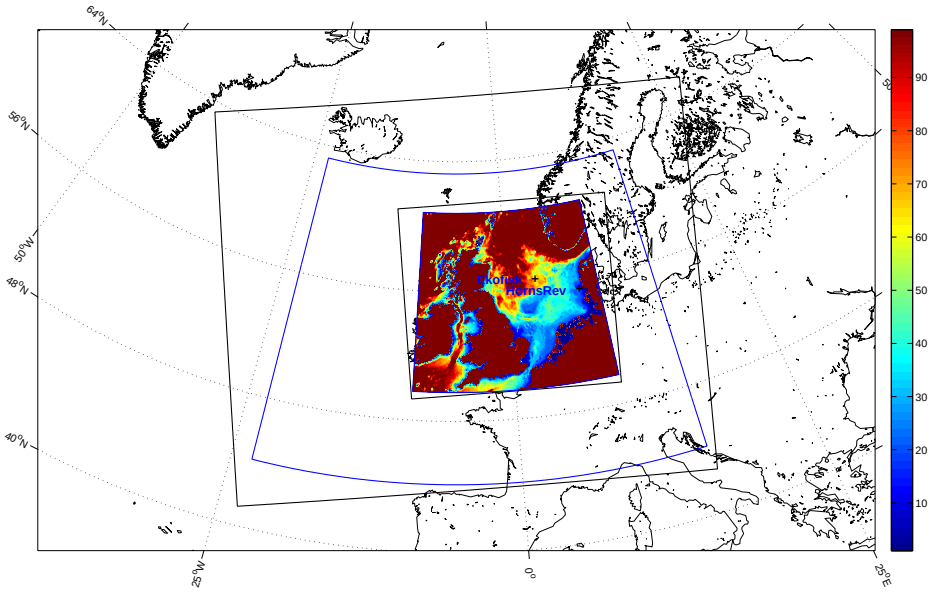

Fig. 2. Model domains for the experiments (EXP1-EXP6) as well as the locations of the measurements at Ekofisk and Horns Rev. The black boxes are WRF domains, and the blue boxes are SWAN domains. The colored area is the depth at SWAN innermost domain.

3 Results

3.1 Spatial distribution

Fig. 4 shows a snapshot of $10m$ wind speeds and directions in comparison with NASA's Quick Scatterometer (QuikScat) data at time $18:40, UTC, 29^{th}Dec.$, 2002,$19:00, UTC, 14^{th}Dec.$, 2003, and $19:20, UTC, 19^{th}Mar.$, 2004. The QuikScat data are of $25km$ resolution, which is too coarse to capture the cell structure as present in storm NW03 (Middle column in Fig.4), as shown by the cloud type

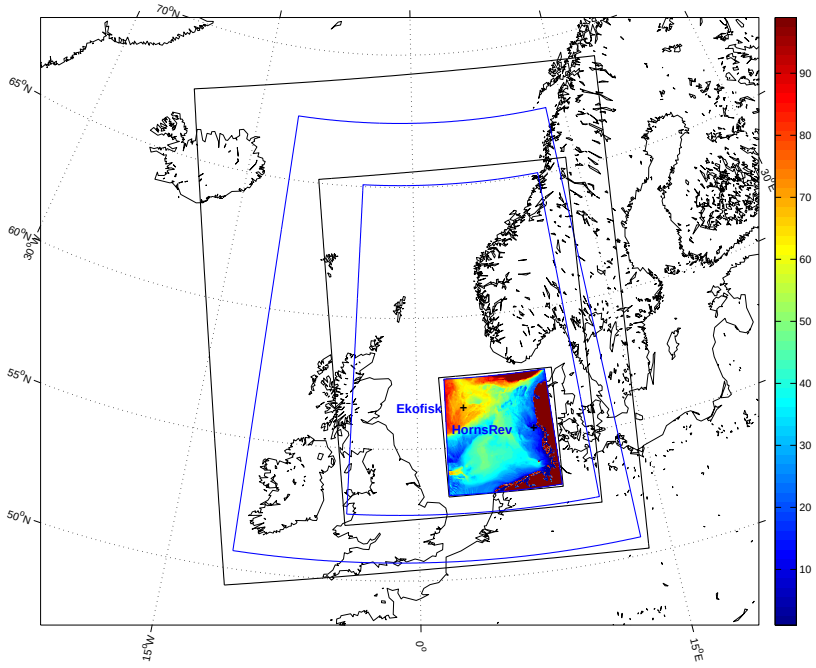

Fig. 3. Model domains for the experiments (EXP7-EXP9) as well as the locations of the measurements at Ekofisk and Horns Rev. The black boxes are WRF domains, and the blue boxes are SWAN domains. The colored area is the depth at SWAN innermost domain.

of horizontal wind pattern at this time. It could be seen that the model in general captures the storm structure well. Wind structures close to the domain boundaries are not always in good agreement where the uncertainty in the modeled data is high. The response of the spatial wind distribution to the different $z_0$methods is not immediately obvious.

3.2 Time Series

The wind speed at measurement height and the significant wave heights are presented for one open ocean site Ekofisk (Fig.5) and one coastal relatively shallow water site Horns Rev(Fig.6). The water depth at the two sites are $66m$ and $10m$ respectively. The high resolution runs improve the model results in both wind speed ($10m$ at Ekofisk and $15m$ at Horns Rev) and significant wave height, especially for the coastal site at Horns Rev (Fig.6(d)). The influence of different z_0 expressions are not obvious at the coastal site where the sea state are not very high (Significant wave height under $3m$). But when it comes to the open ocean site, where the sea state are higher (Significant wave height higher than $4m$), the influence of z_0 expressions become more significant. The Janssen (1991) expression tended to intensify the significant wave height and wind speed during the peak of storm SE02 and NW03 at Ekofisk(Fig.5(a-d)). Since the modeled H_{m0} are lower than measurements in these two cases, using the coupled Janssen (1991) z_0 expression give more accurate H_{m0} than the others. During storm SE02, the modeled $10m$ wind speed are on average higher than measurements at Ekofisk(Fig.5(a)). On the contrary, the modeled H_{m0} are on average lower than measurements(Fig.5(b)). Such phynomenon is also found in NW03 (Fig.5(c,d)). It becomes much better after the resolution increased to $2km$. As shown in Fig.5(e, f) and Fig.6(e, f), storm SW04 has two peaks. The $10m$ wind speed changes fast

Table 1. Design of the experiments relating to the spatial resolution and $z_0$expressions

Name	WRF resolution	SWAN resolution	z_0	Coupling	WRF input	Stroms
EXP1	$25km$	$\sim 12km$	Fairall et al. (2003)	Off	FNL	SE02,NW03,SW04
EXP2	$5km$	$\sim 6km$	Fairall et al. (2003)	Off	FNL	SE02,NW03,SW04
EXP3	$25km$	$\sim 12km$	Fan et al. (2012)	On	FNL	SE02,NW03,SW04
EXP4	$5km$	$\sim 6km$	Fan et al. (2012)	On	FNL	SE02,NW03,SW04
EXP5	$25km$	$\sim 12km$	Janssen (1991)	On	FNL	SE02,NW03,SW04
EXP6	$5km$	$\sim 6km$	Janssen (1991)	On	FNL	SE02,NW03,SW04
EXP7	$2km$	$\sim 1.3km$	Fairall et al. (2003)	Off	CFSR	NW03
EXP8	$2km$	$\sim 1.3km$	Fan et al. (2012)	On	CFSR	NW03
EXP9	$2km$	$\sim 1.3km$	Janssen (1991)	On	CFSR	NW03

between the two peaks. The coupling system doesn't perform well during those fast changing winds. Such phynomenon is also found in storm SE02 around $00:00, UTC, 23^{nd} Dec.2002$ (Fig.5(a)) and storm NW03 around $12:00, UTC, 14^{nd} Dec.2003$ (Fig.5(c) and Fig.6(c)).

4 Conclusions and discussion

Validation of modeled wind and wave fields using the nested COAWST system with point measurements as well as QuikScat data suggest the following: 1) The modelling system as implemented here performs better for storms of certain strcture than the other (it performs better for storms from the west than for storms from the north). 2) The storm wind field favors from the nested, high resolution modeling as well as input of high resolution data. 3) The system is more challenged by fast changing wind conditions. 4) Using Janssen (1991) z_0 expression gives better results of the significant wave hight. Further investigation will focus on the following issues: 1) use higher resolution tests for the coastal zone. 2) include more severe storms. 3) examine heat exchange 6) include ocean model.

5 Acknowledgment

This study is funded mainly by the Danish Forskel project X-WiWa (PSO-12020). The second and third authors acknowledge the EU INNWIND project for the support. QuickScat data for the three storms are provided by Ioanna Karagali.

References

1. Amante, C., & Eakins, B. W. (2009). ETOPO1 1 arc-minute global relief model: procedures, data sources and analysis (p. 19). US Department of Commerce, National Oceanic and Atmospheric Administration, National Environmental Satellite, Data, and Information Service, National Geophysical Data Center, Marine Geology and Geophysics Division.
2. Bolaños, R., Larsén, X., Petersen, O., Nielsen, J., Kelly, M., Kofoed-Hansen, H., Du, J., Sørensen, O., Larsén, S., Hahmann, A., & Badger, M. (2014). Coupling atmosphere and waves for coastal wind turbine design. Coastal Engineering Proceedings, 1(34), management.33. doi:http://dx.doi.org/10.9753/icce.v34.management.33
3. Drennan, W. M., Taylor, P. K., & Yelland, M. J. (2005). Parameterizing the sea surface roughness. Journal of physical oceanography, 35(5), 835-848.
4. Fan, Y., Lin, S. J., Held, I. M., Yu, Z., & Tolman, H. L. (2012). Global ocean surface wave simulation using a coupled atmosphere-wave model. Journal of Climate, 25(18), 6233-6252.
5. Fairall, C. W., Bradley, E. F., Hare, J. E., Grachev, A. A., & Edson, J. B. (2003). Bulk parameterization of air-sea fluxes: Updates and verification for the COARE algorithm. Journal of climate, 16(4), 571-591.

6. Ioc, I. (2008). BODC, 2003. Centenary Edition of the GEBCO Digital Atlas, published on CD-ROM on behalf of the Intergovernmental Oceanographic Commission and the International Hydrographic Organization as part of the General Bathymetric Chart of the Oceans. British oceanographic data centre, Liverpool.
7. Janssen, P. A. E. M.(1991). Quasi-linear theory of wind-wave generation applied to wave forecasting. Journal of Physical Oceanography, 21(11), 1631-1642.
8. Janssen, P. A. E. M.(1992). Consequences of the effect of surface gravity waves on the mean air flow. In Breaking Waves (pp. 193-198). Springer Berlin Heidelberg.
9. Larson, J., Jacob, R., & Ong, E. (2005). The Model Coupling Toolkit: A new Fortran90 toolkit for building multiphysics parallel coupled models. International Journal of High Performance Computing Applications, 19(3), 277-292.
10. Nakanishi, M., & Niino, H. (2009). Development of an improved turbulence closure model for the atmospheric boundary layer. Journal of the Meteorological Society of Japan.Ser. II, 87(5), 895-912.
11. Olabarrieta, M., Warner, J. C., Armstrong, B., Zambon, J. B., & He, R. (2012). Ocean–atmosphere dynamics during Hurricane Ida and Nor'Ida: an application of the coupled ocean–atmosphere–wave–sediment transport (COAWST) modeling system. Ocean Modelling, 43, 112-137.
12. Oost, W. A., Komen, G. J., Jacobs, C. M. J., & Van Oort, C. (2002). New evidence for a relation between wind stress and wave age from measurements during ASGAMAGE. Boundary-Layer Meteorology, 103(3), 409-438.
13. QuikScat data are produced by Remote Sensing Systems and sponsored by the NASA Ocean Vector Winds Science Team. Data are available at www.remss.com.
14. Shchepetkin, A. F., & McWilliams, J. C. (2005). The regional oceanic modeling system (ROMS): a split-explicit, free-surface, topography-following-coordinate oceanic model. Ocean Modelling, 9(4), 347-404.
15. Skamarock, W. C., Klemp, J. B., Dudhia, J., Gill, D. O., Barker, D. M., Wang, W., & Powers, J. G. (2005). A description of the advanced research WRF version 2 (No. NCAR/TN-468+ STR). National Center For Atmospheric Research Boulder Co Mesoscale and Microscale Meteorology Div.
16. Taylor, P. K., & Yelland, M. J. (2001). The dependence of sea surface roughness on the height and steepness of the waves. Journal of physical oceanography, 31(2), 572-590.
17. Warner, J. C., Sherwood, C. R., Signell, R. P., Harris, C. K., & Arango, H. G. (2008). Development of a three-dimensional, regional, coupled wave, current, and sediment-transport model. Computers & Geosciences, 34(10), 1284-1306.
18. Warner, J. C., Armstrong, B., He, R., & Zambon, J. B. (2010). Development of a coupled ocean–atmosphere–wave–sediment transport (COAWST) modeling system. Ocean modelling, 35(3), 230-244.
19. Zambon, J. B., He, R., & Warner, J. C. (2014). Investigation of hurricane Ivan using the coupled ocean–atmosphere–wave–sediment transport (COAWST) model. Ocean Dynamics, 64(11), 1535-1554.

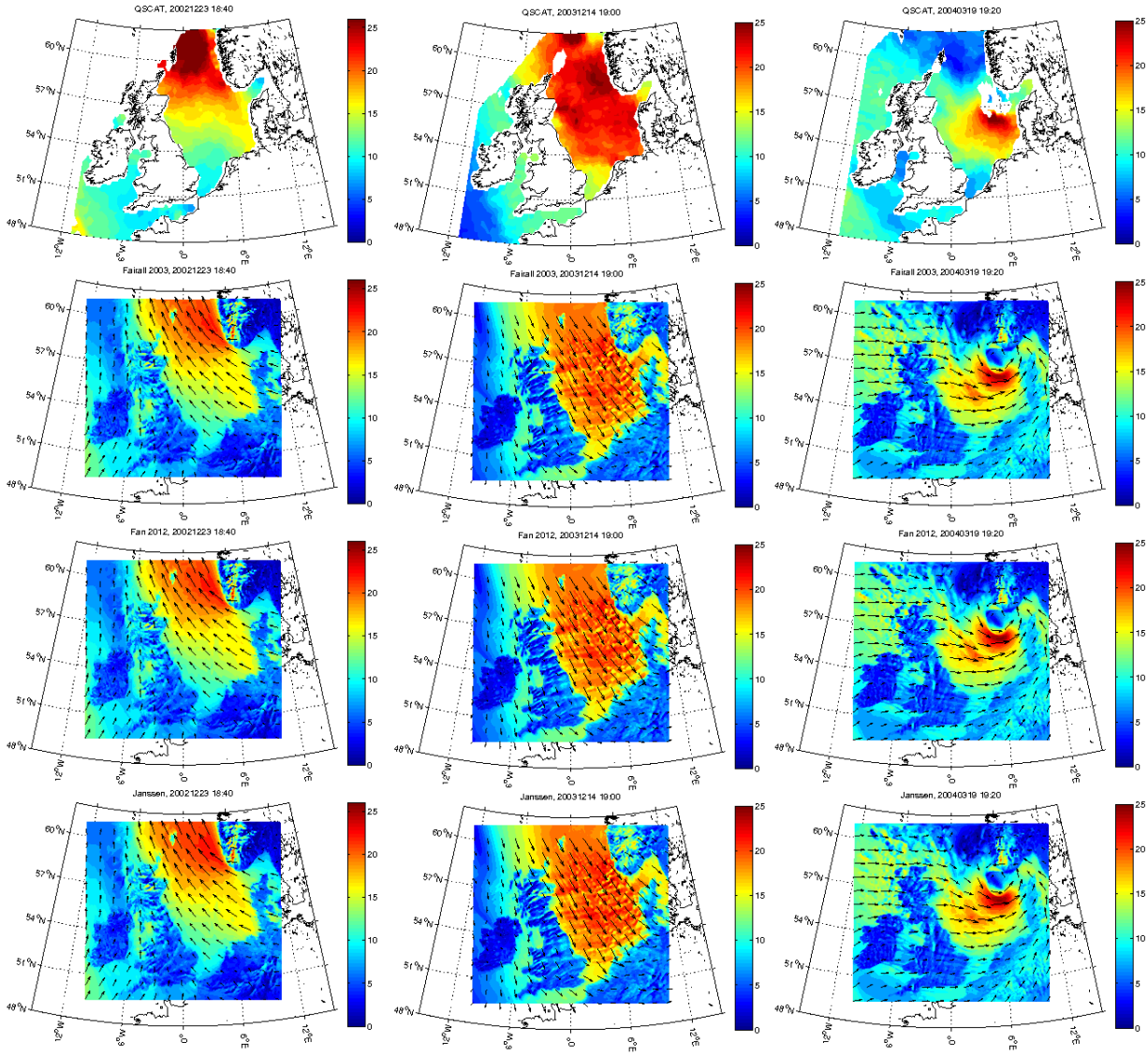

Fig. 4. Snapshot of wind intensities and directions in comparison with QuikScat data. The rows from top to bottom are from QuikScat data, modeled data by EXP2, EXP4, and EXP6. The columns from left to right are strom SW02, NW03, SW04 respectively.

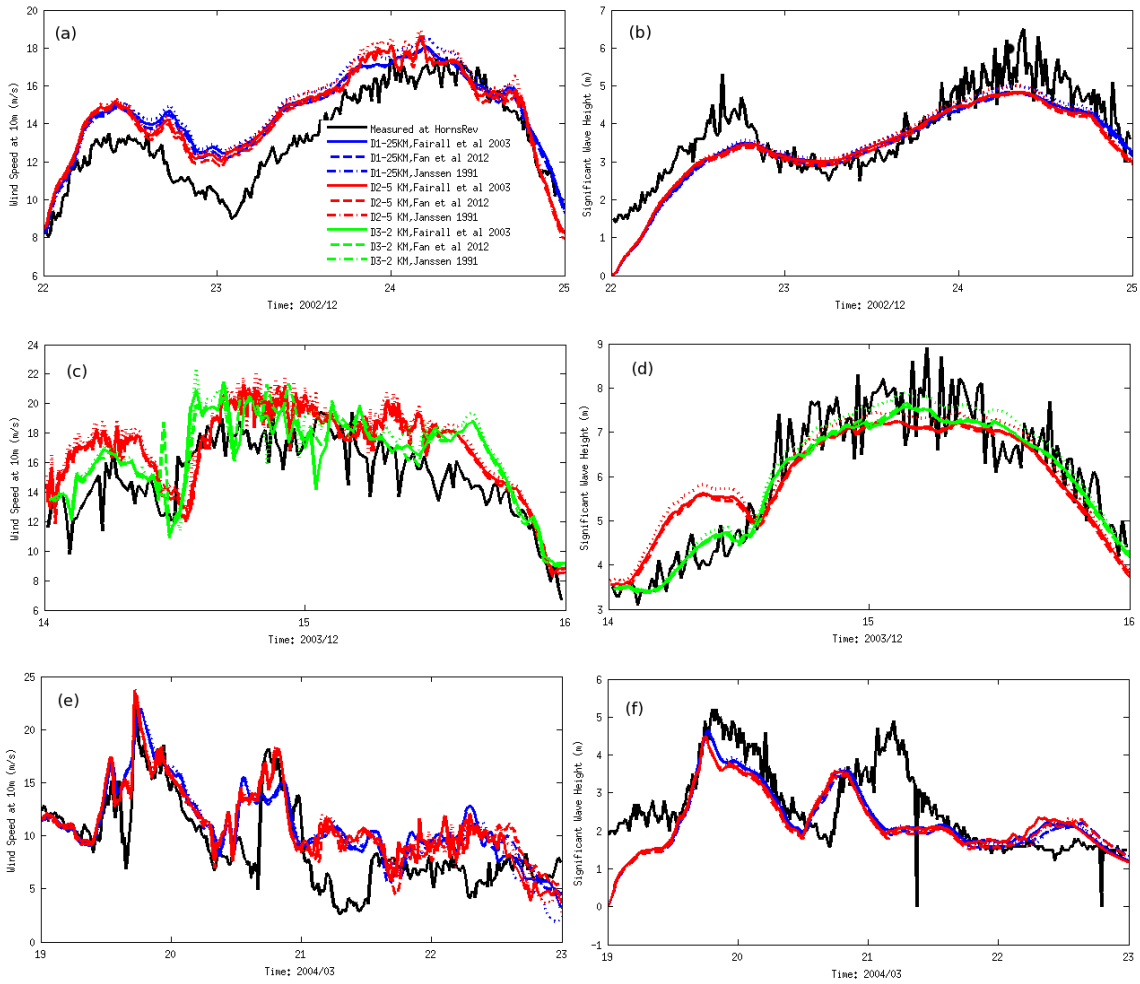

Fig. 5. Time series of the three storms at Ekofisk. The left column are the $10m$ wind speed. The right column are the significant wave height. The rows from top to bottom are strom SW02, NW03, SW04 respectively. For storm SW02 and SW04, EXP1-EXP6 are compared. For storm SW03, EXP2, EXP4, and EXP6-EXP9 are compared.

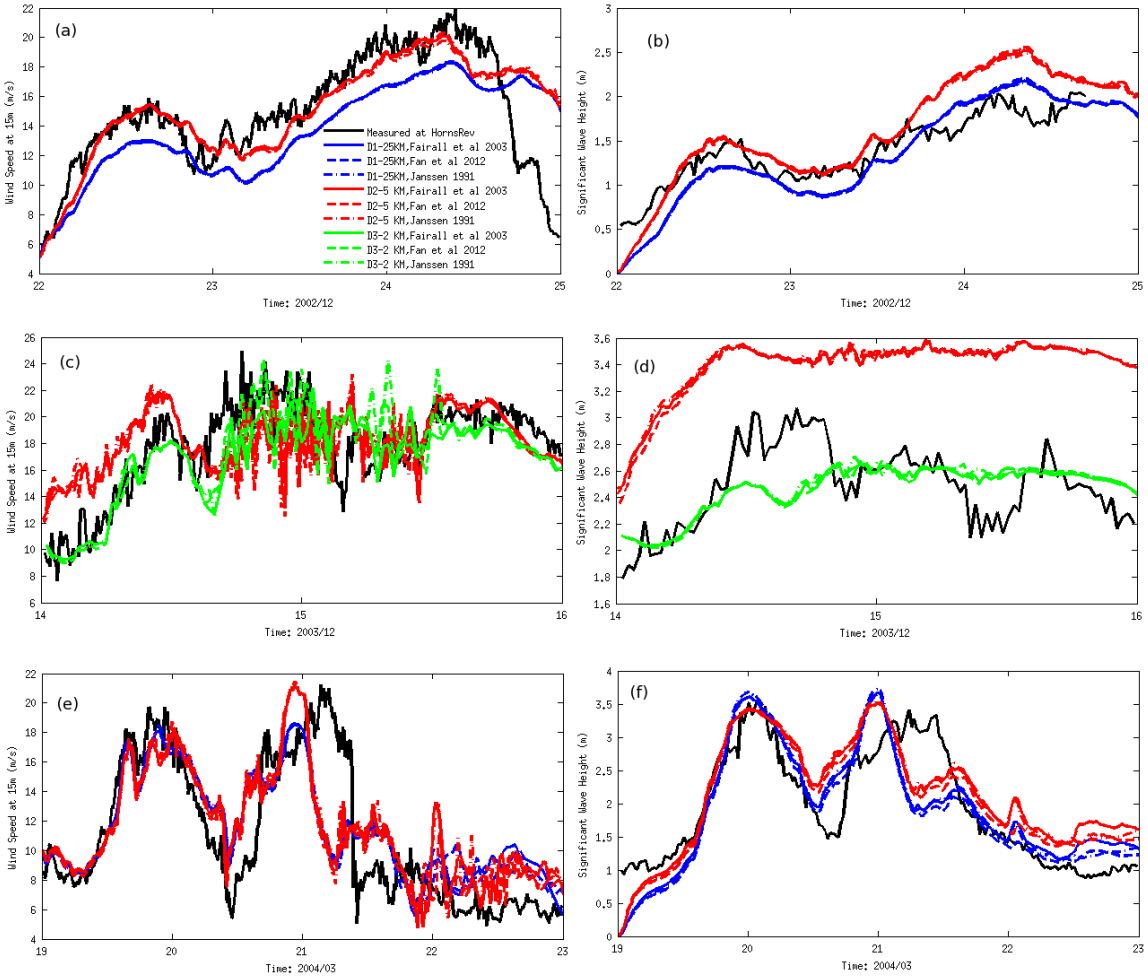

Fig. 6. Time series of the three storms at Horns Rev. The left column are the $15m$ wind speed. The right column are the significant wave height. The rows from top to bottom are strom SW02, NW03, SW04 respectively. For storm SW02 and SW04, EXP1-EXP6 are compared. For storm SW03, EXP2, EXP4, and EXP6-EXP9 are compared.